Pharm Res (2012) 29:2833–2844
DOI 10.1007/s11095-012-0775-8

RESEARCH PAPER

Meta-analysis of Nanoparticulate Paclitaxel Delivery System Pharmacokinetics and Model Prediction of Associated Neutropenia

Sihem Ait-Oudhia • Robert M. Straubinger • Donald E. Mager

Received: 22 January 2012 / Accepted: 1 May 2012 / Published online: 17 May 2012

ABSTRACT

Purpose Nanoparticulate paclitaxel carriers have entered clinical evaluation as alternatives to the Cremophor-based standard Taxol® (Cre-pac). Their pharmacokinetics (PK) is complex, and factors influencing their pharmacodynamics (PD) are poorly understood. We aimed to develop a unified quantitative model for 4 paclitaxel carriers that captures systems-level PK, predicts micro-scale PK processes, and permits correlations between carrier properties and observed PD.

Methods Data consisting of 54 PK profiles and 574 observations were extracted from 20 clinical studies investigating Cre-pac, albumin-(A-pac), liposome-(L-pac), and tocopherol-(T-pac) nanocarriers. A population-PK approach was used for data analysis. All datasets were simultaneously fitted to produce a unified model. Model-based simulations explored relationships between predicted PK and myelosuppression for each formulation.

Results The final model employed nonlinear drug-binding mechanisms to describe Cre-pac and a delayed-release model for A-pac, L-pac, and T-pac. Estimated drug-release rate constants (h^{-1}): Cre-pac (5.19), L-pac (1.26), A-pac (0.72), T-pac (0.74). Simulations of equivalent dosing schemes ranked neutropenia severity (highest to lowest): T-pac~Cre-pac>L-pac~A-pac and predicted remarkably well the clinically-observed relationships between neutropenia and free drug exposure relative to a threshold concentration.

Conclusions Paclitaxel disposition was well-described for all formulations. The derived model predicts toxicodynamics of diverse paclitaxel carriers.

KEY WORDS drug delivery · meta-analysis · neutropenia · paclitaxel · pharmacokinetics

INTRODUCTION

The taxanes are employed as first or second-line therapy for numerous cancers. Because of the high lipophilicity and poor solubility of paclitaxel in pharmaceutical excipients, the first-in-class clinical standard Taxol® (Cre-pac) employs a Cremophor EL (CreEL):ethanol vehicle (1). Cre-pac is usually administered at a dose of 175 mg/m^2 by 3 h infusion. Patients are pre-medicated with corticosteroids and antihistamines to reduce the incidence of serious hypersensitivity reactions to CreEL (2,3). CreEL also influences paclitaxel pharmacokinetics (PK) (4) and contributes to additional side effects of Cre-pac, including peripheral sensory neuropathy (5), alopecia, myalgias, arthralgias, and acute pulmonary reactions (6).

Cre-pac circulates as a microemulsion. Reversible partitioning of paclitaxel into the circulating CreEL

Electronic supplementary material The online version of this article (doi:10.1007/s11095-012-0775-8) contains supplementary material, which is available to authorized users.

S. Ait-Oudhia · R. M. Straubinger · D. E. Mager
Department of Pharmaceutical Sciences
University at Buffalo
State University of New York
Buffalo, New York, USA

S. Ait-Oudhia (✉)
Department of Pharmaceutical Sciences
University at Buffalo, State University of New York
430 Kapoor Hall Buffalo, New York 14214, USA
e-mail: sihema@buffalo.edu

emulsion reduces the fraction of free[1] drug, the form available for tumor penetration, thus contributing to nonlinear dose-dependent antitumor activity (1). CreEL toxicity and its impact on taxane PK and pharmacodynamics (PD) have sustained an intensive search for formulation alternatives, and numerous drug delivery systems have entered clinical trial or use to improve taxane efficacy and tolerability. Several formulations show beneficial effects and possible superiority to Taxol®. However, no quantitative or theoretical basis exists for comparing the efficacy and toxicity of alternative formulations, nor for guiding clinical selection. Head-to-head comparisons among promising formulations are unlikely, and trials generally reference Taxol®. Our objective was to create a quantitative framework to permit investigation and comparison of relationships among: formulation physicochemical properties, *in vivo* characteristics, and the micro-scale- and systems-level PK processes that ultimately drive the observed pharmacodynamics.

Sufficient clinical data exists to compare Cre-pac with 3 alternative formulations. A-pac (Abraxane®) is a microparticulate suspension of paclitaxel bound non-covalently to human albumin. It has a mean particle diameter of 130–150 nm (7). The maximal tolerated dose (MTD) for A-pac is higher than for Taxol®, and A-pac is approved at a recommended dose of 260 mg/m^2 given by 30-min infusion (8). The albumin carrier reportedly facilitates paclitaxel biodistribution by mediating transcytosis from blood to tumor via the gp60 albumin receptor of vascular endothelial cells and enhancing tumor deposition by interaction with the albumin-binding SPARC protein, which is elevated in tumors (9). In phase III clinical trials, A-pac treatment was associated with a greater response rate, a longer time to progression, and prolonged survival compared to Cre-pac (10). SPARC-positive patients had somewhat better response rates (11). PK has been reported for A-pac (8,12,13), and a crossover study with Cre-pac reported free (unbound) plasma paclitaxel concentrations for both formulations (14), permitting comparative estimation of drug release rates.

L-pac (LEP-ETU®) consists of paclitaxel in 150 nm liposomes (15). In a comparison with Cre-pac, the MTD of L-pac was higher and dose-limiting toxicities were less severe (16). The recommended dose is 300 mg/m^2 by 1.5 h infusion. Only total blood PK was reported for L-pac. Preclinical studies of similar liposome-based formulations in rats concluded that paclitaxel release from the carrier was rapid but not instantaneous following iv administration (17).

T-pac (Tocosol® Paclitaxel) is a nanoemulsion containing paclitaxel within 40–80 nm droplets (18,19). Animal studies suggested a more favorable and predictable PK profile for T-pac, and that the nanoemulsion enhances tumor drug deposition (20). Clinically, T-pac was well-tolerated without premedication at 175 mg/m^2 by 15 min infusion (21). Although T-pac demonstrated favorable antitumor activity in cancer patients refractory to prior chemotherapy (22), toxicity was somewhat higher than for Cre-pac, and it was reported to have failed a non-inferiority trial of response rates compared to Cre-pac (23). Available PK data for T-pac include total-blood- and free plasma drug concentrations (21).

The ultimate objective of a unified quantitative analysis of different drug carrier formulations would be to relate physicochemical carrier properties and *in vivo* behavior to pharmacodynamic differences among them. Anti-tumor efficacy is the key objective endpoint of interest, and peripheral sensory neuropathy represents the dose-limiting toxicity of paclitaxel. However, clinical data for those endpoints are not consistently available. In contrast, neutropenia is a commonly-reported biomarker of paclitaxel toxicity (24). A quantitative link between paclitaxel PK and %decrease in absolute neutrophil count (ANC) has been established (24); it correlates with the duration that free plasma paclitaxel remains above an empirically-determined threshold concentration (C_T) of 0.05 μM (24). Neutropenia severity varies among the formulations analyzed here, suggesting that differences in micro-scale- and systems-level PK mediate pharmacodynamic differences. Under their recommended regimens, a higher incidence of grade 4 neutropenia was observed for T-pac compared to Cre-pac (23), L-pac (16), and A-pac (13).

Our objective was to develop a unified model that could simultaneously describe the clinically-observed PK of paclitaxel within 4 physicochemically-related carriers, to test the hypothesis that quantitative differences in paclitaxel exposure for each carrier could explain their clinically-observed pharmacodynamics. Specifically, we hypothesized that a unifying relationship exists among: (*i*) the pharmacokinetics of free- and total- paclitaxel, (*ii*) the estimated carrier drug release rate, and (*iii*) the clinically-observed neutropenia. Our approach was to base the model upon reasonable assumptions that are supported by literature wherever specific experimental data were lacking. The result was a quantitative model whose predictions correlate well with published clinical experience.

[1] Here "free" drug refers to paclitaxel that is not bound to serum proteins or the carrier. Drug released from the carrier exists as both protein-bound- and free (unbound) drug fractions and is referred to as "released".

MATERIALS AND METHODS

Paclitaxel Formulations

Published clinical data were sufficient for comparative evaluation of 4 nano/micro-particulate paclitaxel formulations. Cre-pac (Taxol®) contains 6 mg/ml paclitaxel, 527 mg/ml purified CreEL and 49.7 % (v/v) alcohol. L-pac (LEP-ETU®) apparently consists of phosphatidylcholine:cardiolipin:cholesterol liposomes having a drug:lipid ratio of 1:33 (15). A-pac (Abraxane®) consists of paclitaxel associated with human serum albumin particles; reconstituted it contains 5 mg/mL paclitaxel and 45 mg/mL albumin (7). T-pac (Tocosol® Paclitaxel) consists of 0.5–1 % (w/w) paclitaxel in a mixture of α-tocopherol, polyethyleneglycol-400, α-tocopherylpropylethyleneglycol-1000 succinate, and poloxamer407 (18,19).

Available Clinical Data

Clinical data consisted of 20 studies (Table I) in which paclitaxel was administered by iv infusion with varying doses and infusion times. Data were extracted by digitization. Paclitaxel concentrations were reported as mean data from multiple patients (8,12,13,21,25–30), as individual PK profiles from representative patients that were averaged (14,24,31,32), or as unique PK profiles from representative patients (4,16,33–36). Original supporting data could not be obtained for some publications. Therefore, all data were converted to mean data. The final pooled dataset consisted of 54 PK profiles (Supplementary Fig. S1-3) and 574 observations extracted from: 14 studies with Cre-pac, 6 with A-pac, 2 with L-pac, and 1 with T-pac. Across the studies, concentration-time data for free drug, a key performance parameter that reflects drug release rate from the particle, was available for only Cre-pac, A-pac (14), and T-pac (21). The PK of the carrier itself was available for Cre-pac, but was estimable for L-pac from published data for similar liposomes (37). The dose of CreEL was calculated from the administered paclitaxel dose and the published paclitaxel: CreEL ratio for Taxol®. Over the period in which the studies were conducted (1995–2011), analytical techniques employed for measurement of CreEL and total- *vs.* unbound paclitaxel evolved. In most cases, liquid chromatography/tandem mass spectrometry was used for drug quantification. The limit of quantification for paclitaxel was 1 ng/ml in free plasma for most studies, except (21) in which the limit was 0.1 ng/ml for unbound drug, and 5 ng/ml for total blood concentrations. The lower limit of CreEL detection in plasma was 0.005 % (v/v) (32,38).

Table I Clinical Studies Included in Population Pharmacokinetic Meta-analysis for Paclitaxel

Delivery system	Dose levels (mg/m^2)	Infusion time (h)	Experimental data available	Reference
Cre-pac	175	3	Mean	(21)
Cre-pac	225, 250	1	Mean	(27)
Cre-pac	135, 175, 225	3	Mean	(26)
Cre-pac	175	3	Averaged individual	(14)
A-pac	260	0.5	Averaged individual	
A-pac	135, 200, 300, 350	0.5, 3	Mean	(8)
A-pac	260	0.5	Mean	(12)
Cre-pac	175	3	Mean	
A-pac	130, 200, 260	0.5	Mean	(25)
A-pac	200, 260, 300	0.5	Mean	(13)
A-pac	80, 100, 125, 150, 175, 200	0.5	Mean	(29)
Cre-pac	256	3	Representative individuals	(4)
Cre-pac	225	3	Averaged individual	(31)
Cre-pac	175	3, 6, 24	Mean	(30)
Cre-pac	175	3	Representative individuals	(33)
Cre-pac	175	1, 3, 24	Representative individuals	(36)
Cre-pac	235, 295, 360	3, 24, 96	Representative individuals	(35)
Cre-pac	105, 135, 140, 175	3, 24, 96	Averaged individual	(32)
Cre-pac	135, 175, 225	3, 24	Averaged individual	(24)
Cre-pac	135, 175, 225	3	Representative individuals	(34)
L-pac	80, 100, 120, 140, 160, 180, 200	1	Mean	(28)
L-pac	325	1.5	Representative Individuals	(16)

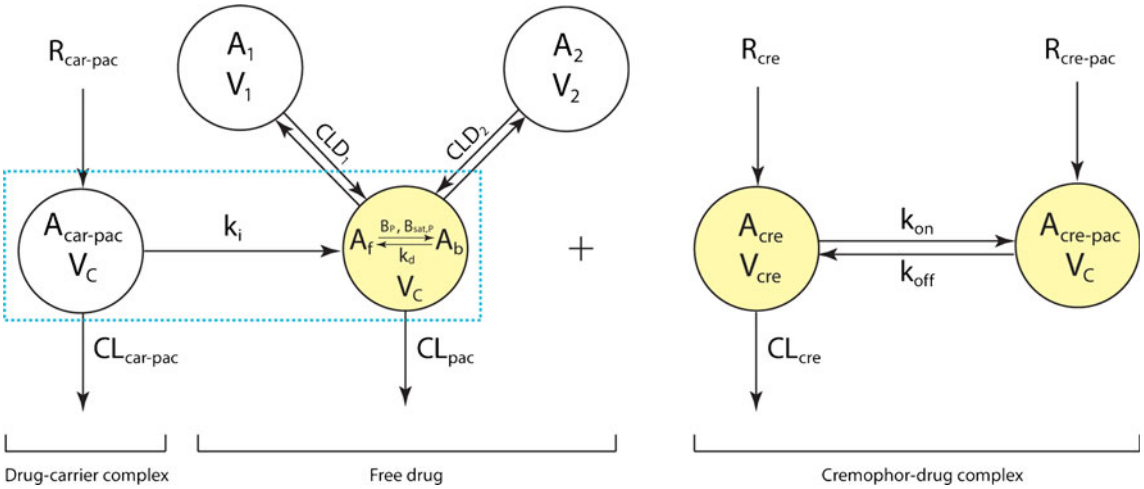

Fig. 1 Final model of paclitaxel pharmacokinetics for Cremophor EL (CreEL)-based formulation (Cre-pac) and 3 nano/microparticulate carriers: liposomes (L-pac), albumin (A-pac) and tocopherol (T-pac). Compartments shaded yellow represent experimentally-measured clinical data used to build and validate the model. Dashed blue rectangle identifies clinically-available data for L-pac, consisting of total blood concentrations only (combined carrier-incorporated, yellow compartment, and released drug, white compartment). Abbreviations are defined in text. Briefly, drug carrier formulations are infused into the blood (R_i), circulating within the compartment $A_{car,pac}$ and releasing drug, which equilibrates between protein-bound (A_b) and unbound (A_f) states, and distributes to peripheral tissues (compartments A_1, A_2). For Cre-pac, CreEL circulates as a microemulsion (A_{Cre}) with which drug in blood equilibrates; CreEL concentration thereby modulates the PK of paclitaxel.

Structural Pharmacokinetic Model

The unified pharmacokinetic model (Fig. 1) was derived by developing individual models that captured characteristics of each formulation, including carrier circulation time, drug release rate or partitioning equilibrium, and biodistribution. From these, a single model was constructed and refined. In the final model, drug input was described as a zero-order process with infusion rate R_i. For L-pac, A-pac, and T-pac, the PK model included a compartment ($A_{car\text{-}pac}$) representing the drug-loaded carrier in blood, from which drug was released via first-order process k_i. The carrier was removed from the circulation with clearance CL_i. Because CreEL comprises a circulating compartment that exchanges drug within plasma, the blood concentration of CreEL impacts paclitaxel PK. Therefore, conceptual elements of a target-mediated drug dispositional (TMDD) model (39) were developed into a 'carrier-mediated drug disposition' (CMDD) component to characterize Cre-pac kinetics. A second-order rate process (k_{on}) described partitioning of free paclitaxel into CreEL. Drug dissociation from CreEL followed a first-order process (k_{off}), analogous to the drug release process for the other carrier formulations. The PK of CreEL micelles was captured by a one-compartment model (A_{cre}) having a volume of distribution V_{cre} and a linear first-order elimination (CL_{cre}).

A three-compartment model was used for the PK of released paclitaxel. It included a central compartment (A_f), having volume of distribution V_c, from which the free fraction of paclitaxel was cleared linearly (CL_{pac}). Two peripheral compartments (A_1, A_2), having volumes V_1, V_2 and intercompartmental clearances CLD_1, CLD_2, served as distribution sites for free paclitaxel. These peripheral compartments were employed so that the model could incorporate elements of a detailed prior analysis of T-pac PK-PD, which hypothesized a 'deep' peripheral compartment associated with toxicity (23).

The final model assumed that the volume of distribution for carrier-associated drug ($A_{car\text{-}pac}$) was equal to V_c, which is a reasonable assumption for particulate drug carriers. In the bloodstream (A_b), constants B_p (linear binding), $B_{sat,p}$ (maximal binding capacity), and K_d (dissociation constant), which were fixed to literature values (21), accounted for the binding of free paclitaxel to plasma proteins and blood cells. All model equations are provided in Supplementary Materials.

Data Analysis

A nonlinear mixed effects modeling approach, implemented in Monolix (v3.1R2, INRIA, France) (40), was used to analyze the PK profiles for all formulations simultaneously. Maximum likelihood estimation was used for estimation of population parameters, which applies the Stochastic Approximation Expectation Maximization algorithm. The between-study variability (BSV) was estimated for parameters $CL_{car\text{-}pac}$, CL_{pac}, CL_{cre}, V_c, V_1, V_2, and V_{cre} assuming a log normal distribution, and exponential residual errors were applied for all model outputs. Owing to a lack of applicable data, the BSV was fixed to zero for k_i and $CL_{car\text{-}pac}$ of T-pac, and k_{on} for Cre-pac.

Simulations of Paclitaxel Profiles, Exposures, and Factors Influencing Pharmacodynamics

Dose or infusion time frequently did not overlap in clinical studies from which data were extracted. Therefore, two types of simulations were carried out using Berkeley Madonna software (v8.3.18, Univ. California, Berkeley) to examine

predictions of the developed model. In the first, mean concentration-time profiles of total- and free drug were generated for all formulations administered via the typical Cre-pac clinical regimen of 175 mg/m^2 paclitaxel infused over 3 h. In the second, exposure to total- and free drug was predicted for the actual regimens reported for each formulation, using a Monte Carlo simulation approach for 100 virtual patients. The simulations provided area-under-the-concentration-time curve ($AUC_{(0-\infty)}$) and predicted mean plasma concentrations with standard deviations.

RESULTS

Pharmacokinetics of Free- and Total Blood Paclitaxel

Figure 1 shows the final derived model, and Fig. 2 shows model fittings to clinical data for total- (Fig. 2a) and free paclitaxel (Fig. 2b) for each delivery system, and CreEL (Fig. 2c). Although the formulations were administered under different regimens in numerous trials and different patient populations, the unified model fit the data well (Fig. S1-3) based on both visual inspection and multiple quantitative goodness-of-fit criteria (Fig. S4-5). All PK parameters were estimated with good precision (Table II), and the estimated BSV was acceptable for all parameters.

The model was used to estimate the paclitaxel release rate for each carrier, which is a difficult-to-quantify performance characteristic that is seldom measured directly, yet is essential for understanding the unique biodistributional behavior of each vehicle and its influence on pharmacodynamics. The estimated half-time for drug release was 8 min for Cre-pac, 33 min for L-pac, and approx. 60 min for A-pac and T-pac. The distribution volume of free paclitaxel (V_c) in the central compartment was 5.38 L/m^2. Elimination of carrier-released drug from the central compartment was linear and similar for all formulations (CL_{pac}=23.7 L/h/m^2), but formulations differed in the estimate for clearance of carrier-associated drug. Drug within T-pac ($CL_{T\text{-}pac}$=22.3 L/h/m^2) was cleared 1.5-fold faster than drug within A-pac ($CL_{A\text{-}pac}$=14.6 L/h/m^2) and $CL_{A\text{-}pac}$ was 15-fold faster than estimated for drug within L-pac ($CL_{L\text{-}pac}$=0.978 L/h/m^2). $CL_{L\text{-}pac}$ was fixed using published data for clearance of similar liposomes (37) to avoid parameter identifiability issues. The estimated differences in $CL_{A\text{-}pac}$ and $CL_{L\text{-}pac}$ appear consistent with observed biodispositional differences between Abraxane® and LEP-ETU® that may arise from the reportedly rapid dissociation of the 130 nm A-pac particles to small (10 nm) drug:albumin complexes upon dilution in plasma (41).

Tissue distributions of drug were also estimated. Although the rate of free paclitaxel distribution to the hypothesized deep (A_2) peripheral compartment (23) (cf. Fig. 1; CLD_2) was only 2-fold higher than its distribution to the shallow (A_1) peripheral compartment (cf. Fig. 1, CLD_1), the fitted volumes of those compartments (V_2=97.9 L/m^2 *vs.* V_1=11.7 L/m^2) suggest that 9-fold more paclitaxel would distribute to A_2 than to A_1. Notably, paclitaxel distribution into the A_2 compartment was hypothesized to correlate with the toxic effects of Cre-pac and T-pac (23).

Because free paclitaxel partitions reversibly into circulating CreEL, which acts as a circulating pharmacokinetic 'compartment' that alters paclitaxel blood PK, a nonlinear binding model was employed for Cre-pac. Based upon clinical data for CreEL plasma concentrations (27,30–32,36), the binding constant for paclitaxel to CreEL (k_{on}=5.06 (h·μg/mL)$^{-1}$) was estimated simultaneously with the other parameters. The central volume of distribution for CreEL was consistent with previous estimates (35). The model captured CreEL data well (Fig. 2c), although the clearance predicted here (CL_{Cre}) was 10-fold lower than reported previously (21). In that prior analysis, the CreEL volume of distribution was fixed, whereas here it was estimated using the CMDD model, which may reflect more accurately the inter-relationship between CreEL and paclitaxel concentrations.

Time-Above-Concentration-Threshold as Unified Predictor of Neutropenia for Paclitaxel Formulations

To compare formulation performance under identical dose and infusion conditions, simulations were performed with the unified model to predict total- (Fig. 3a) and free (Fig. 3b) paclitaxel PK profiles. A common Taxol® regimen (175 mg/m^2 paclitaxel by 3 h infusion) was selected. Simulations predicted that total blood concentrations of A-pac and L-pac would be nearly indistinguishable, and higher than for Cre-pac or T-pac during the infusion period, but decreasing more rapidly when the infusion ended (Fig. 3a), driven by clearance of carrier that still contained drug. Simulation also suggested that with equal dose/infusion times, free plasma paclitaxel concentrations achieved with A-pac and L-pac would fall more rapidly than for Cre-pac and T-pac (Fig. 3b).

Overall exposure ($AUC_{(0-\infty)}$) to total- and free drug were also calculated for the simulated equal-dose/infusion-time regimen. Total paclitaxel exposure in blood would be 3–4 times higher for T-pac and Cre-pac than for L-pac and A-pac (Fig. 3c), and the model-estimated values for Cre-pac, L-pac, and A-pac agree well with clinical data for that dose (8,14,16). In contrast, free paclitaxel exposure would be 4-fold higher for A-pac and L-pac than for Cre-pac and T-pac (Fig. 3d), and the values estimated for Cre-pac agree well with published data (14). Interestingly, simulation predicts that exposure to free drug, the species presumably responsible for action at the tumor target, would be higher for A-pac and L-pac than for Cre-pac and T-pac, and thus implies greater efficacy for A-pac and L-pac.

The fidelity with which the final unified model predicts clinically-reported pharmacodynamic endpoints was investigated by evaluating formulation-dependent severity of

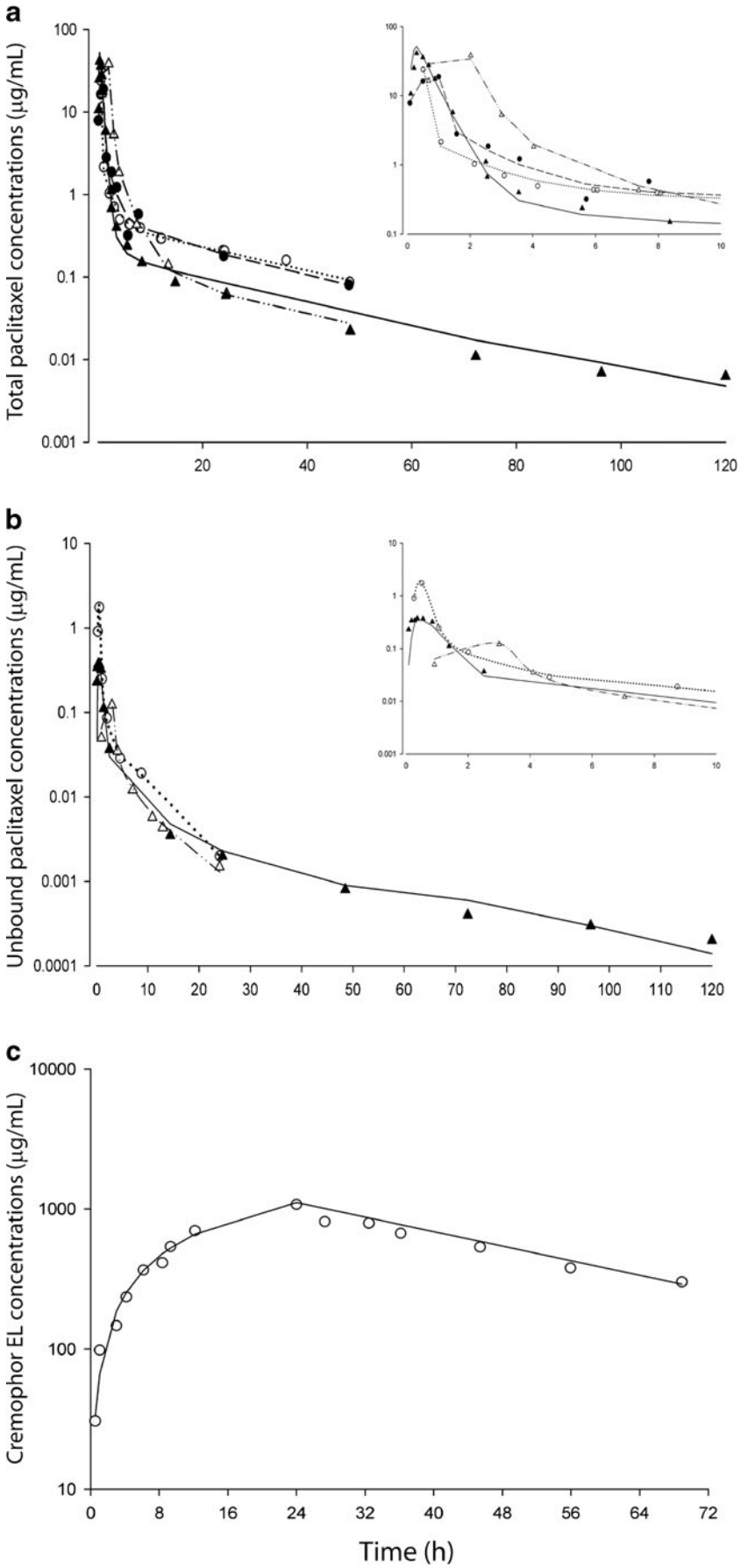
a
Total paclitaxel concentrations (μg/mL)
b
Unbound paclitaxel concentrations (μg/mL)
c
Cremophor EL concentrations (μg/mL)
Time (h)

◀ **Fig. 2** Representative pharmacokinetic profiles of paclitaxel for 4 formulations. Data were extracted from published clinical studies (Table I), and the model of Fig. 1 was refined to fit all data simultaneously. Symbols: observed clinical data for (O) A-pac, (●) L-pac, (Δ) Cre-pac, and (▲) T-pac. Lines: model-predicted concentrations for ····· A-pac, – – – – L-pac, — · — · — Cre-pac, and ——— T-pac. (**a**) T total blood paclitaxel concentrations *versus* time for all formulations; inset shows initial (0–10 h) data and model predictions. (**b**) Unbound (free) paclitaxel concentrations *versus* time. (**c**) Cremophor EL concentrations *versus* time for a 24 h infusion.

neutropenia, a commonly-reported toxicity. Previous studies concluded that neutropenia severity correlates with the duration that free plasma paclitaxel concentrations exceed a threshold concentration (C_T) of 0.05 μM (24,42–44). Figure 3b overlays C_T on a plot of simulated free paclitaxel concentrations for the 4 formulations. A time-above-threshold of 13 h is predicted for A-pac, 16 h for L-pac, 21 h for Cre-pac, and 34 h for T-pac. Notably, given the extended time-above-C_T predicted for T-pac, T-pac toxicity was greater than that of Cre-pac in a phase III trial (23).

Both time-above-C_T (Fig. 3b) and the AUC of free plasma paclitaxel (Fig. 3d) predicted by simulation suggest that neutropenia resulting from L-pac and A-pac should be similar, and that toxicity of T-pac would exceed that of Cre-pac. Figure 4a overlays the predicted time-above-C_T for the 4 formulations (cf. Fig. 3b) upon a previously-published relationship between free-drug time-above-C_T and %decrease in ANC (24). Under identical treatment regimens, the severity of paclitaxel-induced neutropenia for the formulations administered with equivalent doses/infusion times is predicted to conform to the rank order: T-pac>Cre-pac>L-pac~A-pac. As validation of the model, it was possible to predict by simulation the severity of neutropenia that would be observed for the doses and infusion times actually employed in clinical trials. Figure 4b shows the predicted %decrease in ANC overlaid with the reported clinical data for each formulation. Model predictions and clinical data show striking correlations for the 3 formulations for which data exist; data for A-pac are unpublished.

DISCUSSION

Development of alternative delivery approaches for taxanes was motivated initially by poor drug solubility in aqueous and organic excipients, and the serious adverse effects of the Cremophor EL excipient in the clinical standard Taxol®. The diverse strategies pursued to circumvent these challenges have yielded several alternatives. In some cases,

Table II Pharmacokinetic Parameters, Between Study Variability (BSV), Residual Variability (ε_i), and their Percent Relative Standard Errors (%RSE)

Parameter (unit)	Definition	Estimate (%RSE)	BSV[a] (%RSE)
$k_{L\text{-}pac}$ (h^{-1})	First-order release rate constant (L-pac)	1.26 (2.2)	0[b] (NA)
$k_{A\text{-}pac}$ (h^{-1})	First-order release rate constant (A-pac)	0.72 (26.4)	0[b] (NA)
k_{off} (h^{-1})	First-order release rate constant (Cre-pac)	5.19 (131)	0[b] (NA)
$k_{T\text{-}pac}$ (h^{-1})	First-order release rate constant (T-pac)	0.74 (8)	0[b] (NA)
k_{on} ($h.\mu g/mL/m^2)^{-1}$	Second-order binding constant	5.06 (15.8)	0[b] (NA)
V_{cre} (L/m^2)	Central volume of distribution (CreEL)	5.57 (19.7)	0.43 (43.6)
V_C (L/m^2)	Central volume of distribution (unbound paclitaxel)	5.38 (35.3)	0.28 (53.6)
V_1 (L/m^2)	Unbound volume of distribution in peripheral compartment 1	11.7 (38.5)	0.33 (60.2)
V_2 (L/m^2)	Unbound volume of distribution in peripheral compartment 2	97.9 (20.4)	0.17 (63.6)
$CL_{L\text{-}pac}$ ($L/h/m^2$)	Linear clearance (liposomes)	0.978[c](NA)	NA
$CL_{A\text{-}pac}$($L/h/m^2$)	Linear clearance (A-pac)	14.6 (30.2)	0.63 (41.3)
$CL_{T\text{-}pac}$ ($L/h/m^2$)	Linear clearance (T-pac)	22.3 (11)	0[b] (NA)
CL_{cre} ($L/h/m^2$)	Linear clearance (CreEL)	0.0549 (31)	0.48 (54.1)
CL_{pac} ($L/h/m^2$)	Linear clearance (unbound paclitaxel)	23.7 (31.9)	0.43 (30.2)
CLD_1 ($L/h/m^2$)	Intercompartmental clearance	4.17 (33.6)	0.13 (52.6)
CLD_2 ($L/h/m^2$)	Intercompartmental clearance	2.89 (31.8)	0.23 (8.4)
ε1 (%)	Residual variability (total A-pac)	0.769 (3.1)	
ε2 (%)	Residual variability (unbound CreEL)	0.709 (3.2)	
ε3 (%)	Residual variability (unbound paclitaxel)	0.835 (6.6)	
ε4 (%)	Residual variability (total Cre-pac)	0.849 (6.8)	
ε5 (%)	Residual variability (total L-pac)	1.11 (11)	
ε6 (%)	Residual variability (total T-pac)	0.549 (11)	

[a]Estimates are the variances for BSV

[b]Fixed value

[c]Fixed from (37)

NA not applicable

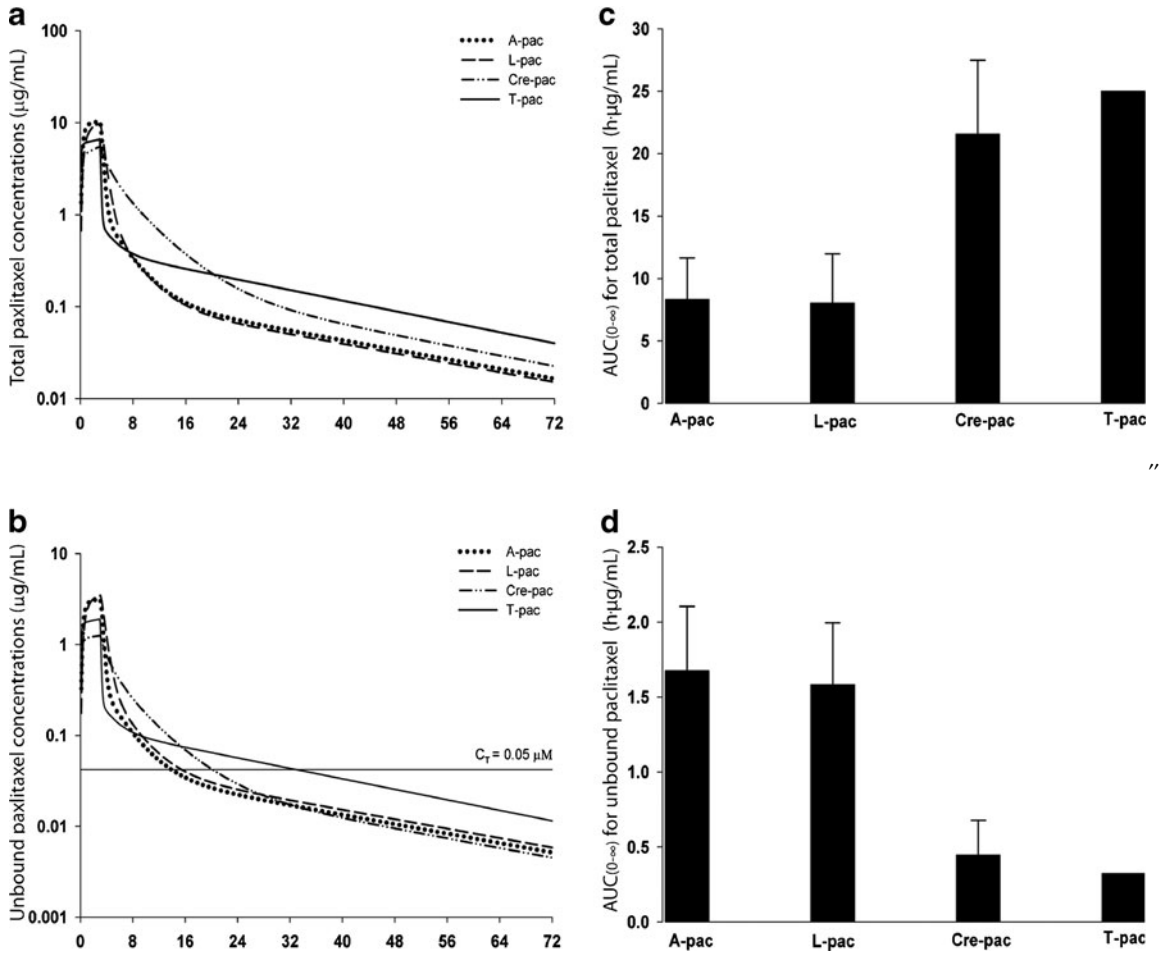

Fig. 3 Model predictions of paclitaxel pharmacokinetic profiles and area-under-the-concentration-time curve ($AUC_{(0-\infty)}$) for all 4 formulations as if given at same dose/infusion time (175 mg/m^2 over 3 h). (**a**) Total blood paclitaxel PK profiles; line patterns denoting formulations are same as in Fig. 2. (**b**) Unbound (free) paclitaxel PK profiles; horizontal line marks empirically-determined threshold concentration (C_T) of 0.05 μM (24) above which neutropenia occurs; (**c**) $AUC_{(0-\infty)}$ for total blood paclitaxel concentrations; (**d**) $AUC_{(0-\infty)}$ for free paclitaxel concentrations. Error bars represent standard deviation from 100 simulated datasets.

carrier systems reduce toxicity and may improve efficacy. In others, toxicity may be elevated, despite promising preclinical results. The development of drug delivery strategies is empirical, and formulation characteristics that enhance efficacy are difficult to discern. Costs of developing new chemical entities vastly exceed development of carrier strategies that improve efficacy by optimizing concentration profiles or biodistribution of existing drugs, thus sustaining interest in oncology drug delivery systems. Quantitative, systems pharmacological analysis could provide a unifying approach for understanding the influence of carrier properties upon clinical performance of chemotherapeutic agents, assist in identifying more promising drug delivery strategies, and inform clinical selection among alternative carriers. Indeed, the *Critical Path Initiative* (45) promulgated by the US Food and Drug Administration emphasizes the need for quantitative modeling and simulation to accelerate the drug development process.

Our primary objective was to develop a quantitative framework for comparison of the pharmacokinetic characteristics of diverse paclitaxel carrier formulations, on both the micro- and systems levels, and gain insight into their clinical impact. A broader objective was to test proof-of-concept that a quantitative and predictive analysis framework could be developed with typical clinical data, which can be sparse and disparate. For paclitaxel delivery vehicles, abundant clinical data are available for Taxol®, and sufficient data exist for Abraxane® and two formulations in earlier-phase clinical development (LEP-ETU® and Tocosol®), to support development of a unified PK model framework. Because the biodistributional properties imposed upon paclitaxel by each carrier drive clinically-important pharmacodynamic endpoints, we imposed two requirements. The first was that in a unified model, the mechanisms to describe paclitaxel release and disposition for all carrier systems would incorporate a minimum of formulation-specific elements. The second was that the final model must capture the PK behavior of each formulation under simultaneous analysis of clinical data for all formulations.

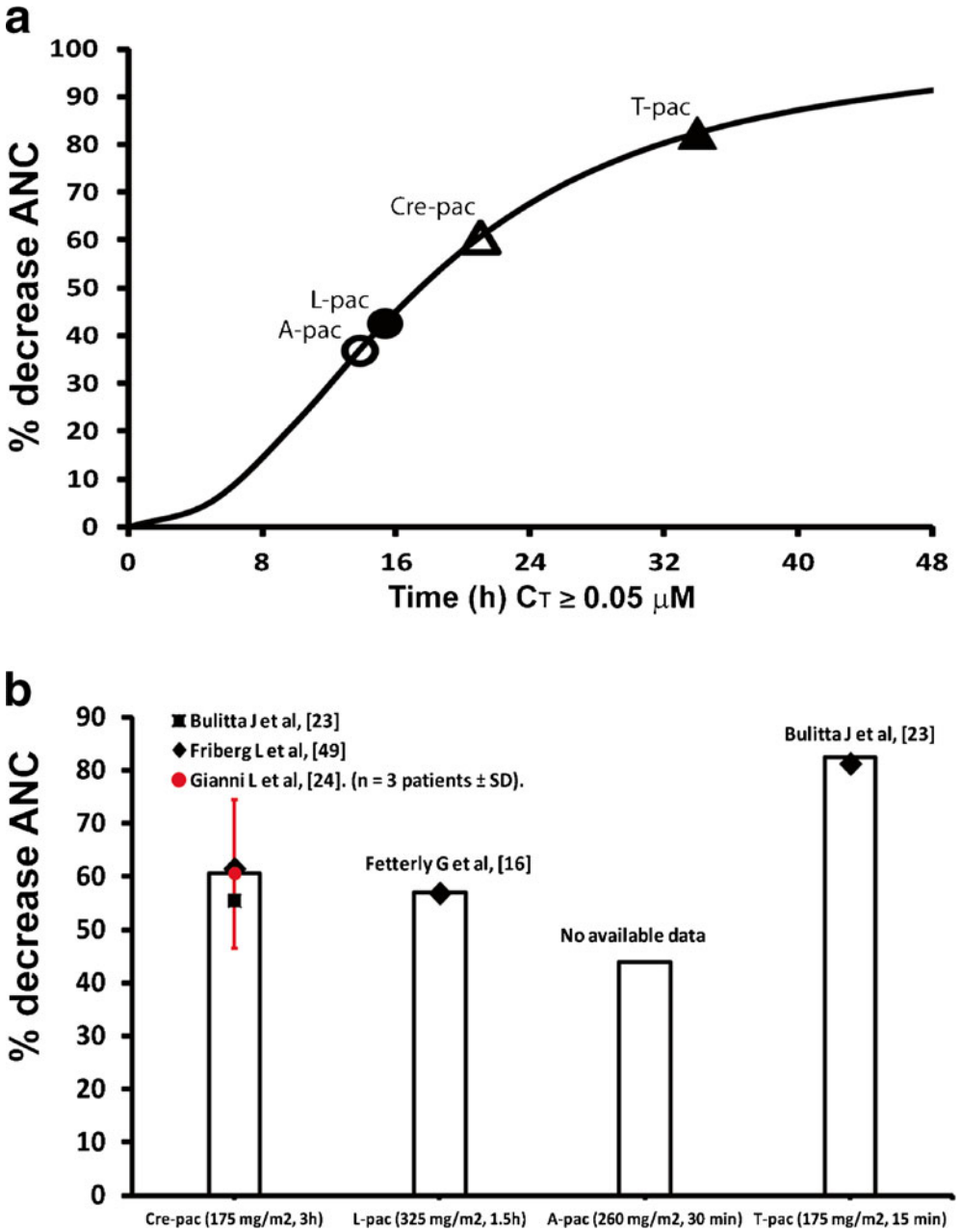

Fig. 4 Model predictions comparing paclitaxel neutrophil toxicity for 4 paclitaxel formulations. (**a**) Abscissa shows free drug time-over-threshold C_T (0.05 μM) calculated from simulation of Fig. 3b, in which PK was estimated as if all formulations were given at same dose/infusion time (175 mg/m^2 over 3 h); symbol is placed on the smooth curve (solid line) representing previously-described relationship between time-over-C_T and %decrease in ANC (ordinate) (24). (**b**) Comparison of model-predicted neutropenia with published clinical data for each formulation. Open bars: model-predicted %decrease in ANC for actual clinical regimen for each formulation (stated below abscissa). Symbols: actual % decrease ANC reported in the cited clinical studies (listed above bar).

By incorporating a small number of reasonable assumptions, the final model is remarkably simple. A key assumption was that PK of carrier-released drug is formulation-independent. A second was that despite considerable physicochemical differences among the delivery systems, only two drug release behaviors were required to capture the data. For A-pac, L-pac, and T-pac, a simple first-order, delayed drug release model was sufficient. For Cre-pac, a CMDD phenomenon was introduced because the drug equilibrates with the circulating CreEL emulsion compartment, and as CreEL is cleared, the volume of the emulsion compartment changes. This is analogous to TMDD effects, in which high-affinity therapeutic ligands and their targets exist at stoichiometrically-comparable concentrations, and target abundance therefore modulates their PK (39).

The unified model captures well the differences in PK behavior of all formulations, and additionally allowed assessment of factors that may underlie formulation-dependent

differences in pharmacodynamics. The PK of free paclitaxel was described successfully using a linear three-compartment model (42). The rate of drug release from the carrier and binding of paclitaxel to CreEL, plasma proteins, and red blood cells are parameters of high importance that influence PK-PD (21) and were estimated successfully. The PK of the carriers themselves was included as a model element, and published data permitted their estimation (Fig. 1). For all formulations and available data, the developed model made excellent predictions of clinically-observed total- and free paclitaxel concentrations, as well as circulating CreEL (Fig. S1-3). The model performed well based upon diagnostic plots (Fig. S4) and internal evaluation (Fig. S5).

The physicochemical characteristics of each carrier determine the kinetics of paclitaxel release and were estimated. For Cre-pac, the drug partitions among: (*i*) the circulating CreEL compartment, (*ii*) plasma-protein bound, and (*iii*) free in blood. This likely explains the rapid release rate estimated for Cre-pac, and the influence of circulating CreEL on drug PK. Paclitaxel release from L-pac and T-pac would be influenced by the thermodynamics of drug incorporation within the liposome bilayer or the tocopherol emulsion. The estimated half-life for drug release from T-pac agrees well with estimates of time for 90 % release to the central compartment (1.14±0.16 h) based on clinical data (21). The slower drug release predicted for A-pac may reflect the affinity of paclitaxel for albumin, which binds approx. 6.6 paclitaxel molecules per molecule (46). For A-pac and T-pac, slower drug release rates would be consistent with the demonstrated feasibility to administer these formulations as more rapid infusions (30 and 15 min, respectively) than used for Cre-pac (3 h). Drug release data are not available for L-pac, but it was given safely by 1.5 h infusion and it was unstated as to whether the drug could be administered more rapidly. A sensitivity analysis shows that changes in the release rate constants influence overall free drug PK profiles for all formulations; however, the time above C_T for L-pac and T-pac formulations are the least sensitive to perturbations in the release rate constant (Fig. S6).

The final model made excellent predictions of drug release rates for those cases in which clinical data were available to confirm them. For all formulations, simulations with the model identified a critical role for free- and total drug PK in determining their toxicodynamics. This underscores the necessity of measuring drug release rates from carrier formulations clinically, which was noted by FDA analysts during the approval process for one particulate paclitaxel carrier formulation (47).

Paclitaxel pharmacodynamics clearly are formulation-dependent. Insufficient data exist at present to extend the developed model to compare therapeutic efficacy. However, available data do permit investigation of relationships between carrier characteristics and toxicity. Clinical reports suggest that A-pac and L-pac are better tolerated than Cre-pac; the reported MTD for A-pac (300 mg/m^2) and L-pac (325 mg/m^2) (8,16) are higher than for Cre-pac (135–200 mg/m^2 (48)). In contrast, neutropenia was more severe with T-pac than with Cre-pac (21,23). Efficacy reported for A-pac was greater than Cre-pac (10), whereas the objective clinical response rate reported for T-pac was lower than for Cre-pac (37 % *versus* 45 %, p=0.085) (23). Simulations with the developed model predicted that whole blood exposures would be higher for Cre-pac and T-pac than for L-pac and A-pac if administered at equivalent doses and infusion times, but that the $AUC_{(0-\infty)}$ of free (unbound) drug would be in reverse order (A-pac~L-pac>Cre-pac~T-pac). If systemic exposure to free paclitaxel drives cytotoxicity at the tumor site, this rank order would be consistent with available clinical data, and would suggest that antitumor potency of A-pac and L-pac should exceed that of Cre-pac and T-pac. Although peak concentrations and $AUC_{(0-\infty)}$ of free drug were highest for A-pac and L-pac, their time-above-threshold was shorter. Clearance of carrier-incorporated drug was estimated to be faster than for Cre-pac and T-pac, and thus drove concentrations more rapidly below the empirically-derived threshold for neutropenia (C_T= 0.05 μM) (24). Remarkably, when the predicted time-above-C_T for each formulation was used to calculate the expected severity of neutropenia (24,42–44), the prediction (Fig. 4b) matched remarkably well with clinical reports for L-pac (16), Cre-pac (23,24,49), and T-pac (23). It bears note that drug release rates for L-pac have not been reported. Thus simulation based on clinical data is the only means to calculate this key performance parameter. That the model predicted correctly the clinically-observed neutropenia for L-pac suggests that parameter estimates for critical but unavailable performance characteristics may be accurate.

In conclusion, a unified pharmacokinetic model was developed that described well the concentration-time profiles of total- and free paclitaxel for 4 different formulations. The model hypothesized two different mechanisms by which drug release behavior influenced biodisposition, but only common disposition processes for free drug were necessary to describe the clinical data for all formulations. Simulation provided the ability to compare formulation characteristics under clinical conditions never investigated, such as identical dose and infusion times, to make predictions that appear consistent with available data on antitumor efficacy, and to predict accurately the magnitude of toxicity expected under the differing administration conditions. Simulations independently confirmed the relationship between free plasma paclitaxel concentration and time-over-threshold of 0.05 μM as a predictor for paclitaxel-induced neutropenia. Finally, experimental measurement of drug release rates clearly is essential for the comparison of carrier-based formulations. With appropriate data, this pharmacometric

approach could accelerate the clinical development of carrier-based formulations of taxanes and other important oncology drugs.

ACKNOWLEDGMENTS AND DISCLOSURES

Support was by unrestricted funds from the UB-Pfizer Strategic Alliance. We gratefully acknowledge the authors of the publications that made this work possible.

REFERENCES

1. ten Tije AJ, Verweij J, Loos WJ, Sparreboom A. Pharmacological effects of formulation vehicles: implications for cancer chemotherapy. Clin Pharmacokinet. 2003;42:665–85.
2. Rowinskyand EK, Donehower RC. Paclitaxel (taxol). N Engl J Med. 1995;332:1004–14.
3. Weiss RB, Donehower RC, Wiernik PH, Ohnuma T, Gralla RJ, Trump DL, *et al.* Hypersensitivity reactions from taxol. J Clin Oncol. 1990;8:1263–8.
4. Sparreboom A, van Zuylen L, Brouwer E, Loos WJ, de Bruijn P, Gelderblom H, *et al.* Cremophor EL-mediated alteration of paclitaxel distribution in human blood: clinical pharmacokinetic implications. Cancer Res. 1999;59:1454–7.
5. Brat DJ, Windebank AJ, Brimijoin S. Emulsifier for intravenous cyclosporin inhibits neurite outgrowth, causes deficits in rapid axonal transport and leads to structural abnormalities in differentiating N1E.115 neuroblastoma. J Pharmacol Exp Ther. 1992;261:803–10.
6. Rowinsky EK, Burke PJ, Karp JE, Tucker RW, Ettinger DS, Donehower RC. Phase I and pharmacodynamic study of taxol in refractory acute leukemias. Cancer Res. 1989;49:4640–7.
7. Stinchcombe TE. Nanoparticle albumin-bound paclitaxel: a novel Cremphor-EL-free formulation of paclitaxel. Nanomedicine (Lond). 2007;2:415–23.
8. Ibrahim NK, Desai N, Legha S, Soon-Shiong P, Theriault RL, Rivera E, *et al.* Phase I and pharmacokinetic study of ABI-007, a Cremophor-free, protein-stabilized, nanoparticle formulation of paclitaxel. Clin Cancer Res. 2002;8:1038–44.
9. Robinsonand DM, Keating GM. Albumin-bound Paclitaxel: in metastatic breast cancer. Drugs. 2006;66:941–8.
10. Gradishar WJ, Tjulandin S, Davidson N, Shaw H, Desai N, Bhar P, *et al.* Phase III trial of nanoparticle albumin-bound paclitaxel compared with polyethylated castor oil-based paclitaxel in women with breast cancer. J Clin Oncol. 2005;23:7794–803.
11. Desai N, Trieu V, Damascelli B, Soon-Shiong P. SPARC expression correlates with tumor response to albumin-bound paclitaxel in head and neck cancer patients. Transl Oncol. 2009;2:59–64.
12. Sparreboom A, Scripture CD, Trieu V, Williams PJ, De T, Yang A, *et al.* Comparative preclinical and clinical pharmacokinetics of a cremophor-free, nanoparticle albumin-bound paclitaxel (ABI-007) and paclitaxel formulated in Cremophor (Taxol). Clin Cancer Res. 2005;11:4136–43.
13. Yamada K, Yamamoto N, Yamada Y, Mukohara T, Minami H, Tamura T. Phase I and pharmacokinetic study of ABI-007, albumin-bound paclitaxel, administered every 3 weeks in Japanese patients with solid tumors. Jpn J Clin Oncol. 2010;40:404–11.
14. Gardner ER, Dahut WL, Scripture CD, Jones J, Aragon-Ching JB, Desai N, *et al.* Randomized crossover pharmacokinetic study of solvent-based paclitaxel and nab-paclitaxel. Clin Cancer Res. 2008;14:4200–5.
15. Zhang JA, Anyarambhatla G, Ma L, Ugwu S, Xuan T, Sardone T, *et al.* Development and characterization of a novel Cremophor EL free liposome-based paclitaxel (LEP-ETU) formulation. Eur J Pharm Biopharm. 2005;59:177–87.
16. Fetterly GJ, Grasela TH, Sherman JW, Dul JL, Grahn A, Lecomte D, *et al.* Pharmacokinetic/pharmacodynamic modeling and simulation of neutropenia during phase I development of liposome-entrapped paclitaxel. Clin Cancer Res. 2008;14:5856–63.
17. Fetterly GJ, Straubinger RM. Pharmacokinetics of paclitaxel-containing liposomes in rats. AAPS PharmSci. 2003;5:E32.
18. Constantinides PP, Tustian A, Kessler DR. Tocol emulsions for drug solubilization and parenteral delivery. Adv Drug Deliv Rev. 2004;56:1243–55.
19. Constantinides PP, Lambert KJ, Tustian AK, Schneider B, Lalji S, Ma W, *et al.* Formulation development and antitumor activity of a filter-sterilizable emulsion of paclitaxel. Pharm Res. 2000;17:175–82.
20. Perez EA. Novel enhanced delivery taxanes: an update. Semin Oncol. 2007;34(suppl 1–5).
21. Bulitta JB, Zhao P, Arnold RD, Kessler DR, Daifuku R, Pratt J, *et al.* Mechanistic population pharmacokinetics of total and unbound paclitaxel for a new nanodroplet formulation *versus* Taxol in cancer patients. Cancer Chemother Pharmacol. 2009;63:1049–63.
22. Bogdanova N, Karaseva N, Ognerubov N, Golubeva O, Weiden P. Paclitaxel injectable emulsion: phase 2a study of weekly administration in patients with non-small lung cancer (NSCLC). J Clin Oncol. (ASCO Annual Meeting Proceedings). 2004;22: abstract No. 7133.
23. Bulitta JB, Zhao P, Arnold RD, Kessler DR, Daifuku R, Pratt J, *et al.* Multiple-pool cell lifespan models for neutropenia to assess the population pharmacodynamics of unbound paclitaxel from two formulations in cancer patients. Cancer Chemother Pharmacol. 2009;63:1035–48.
24. Gianni L, Kearns CM, Giani A, Capri G, Vigano L, Lacatelli A, *et al.* Nonlinear pharmacokinetics and metabolism of paclitaxel and its pharmacokinetic/pharmacodynamic relationships in humans. J Clin Oncol. 1995;13:180–90.
25. Biakhov MY, Kononova GV, Iglesias J, Desai N, Bhar P, Schmid AN, *et al.* nab-Paclitaxel in patients with advanced solid tumors and hepatic dysfunction: a pilot study. Expert Opin Drug Saf. 2010;9:515–23.
26. Brouwer E, Verweij J, De Bruijn P, Loos WJ, Pillay M, Buijs D, *et al.* Measurement of fraction unbound paclitaxel in human plasma. Drug Metab Dispos. 2000;28:1141–5.
27. Brouwer E, Verweij J, Hauns B, Loos WJ, Nooter K, Mross K, *et al.* Linearized colorimetric assay for cremophor EL: application to pharmacokinetics after 1-hour paclitaxel infusions. Anal Biochem. 1998;261:198–202.
28. Lim WT, Tan EH, Toh CK, Hee SW, Leong SS, Ang PC, *et al.* Phase I pharmacokinetic study of a weekly liposomal paclitaxel formulation (Genexol-PM) in patients with solid tumors. Ann Oncol. 2010;21:382–8.
29. Nyman DW, Campbell KJ, Hersh E, Long K, Richardson K, Trieu V, *et al.* Phase I and pharmacokinetics trial of ABI-007, a novel nanoparticle formulation of paclitaxel in patients with advanced nonhematologic malignancies. J Clin Oncol. 2005;23:7785–93.
30. Rischin D, Webster LK, Millward MJ, Linahan BM, Toner GC, Woollett AM, *et al.* Cremophor pharmacokinetics in patients receiving 3-, 6-, and 24-hour infusions of paclitaxel. J Natl Cancer Inst. 1996;88:1297–301.
31. Sparreboom A, Loos WJ, Verweij J, de Vos AI, van der Burg ME, Stoter G, *et al.* Quantitation of Cremophor EL in human plasma samples using a colorimetric dye-binding microassay. Anal Biochem. 1998;255:171–5.
32. van Tellingen O, Huizing MT, Panday VR, Schellens JH, Nooijen WJ, Beijnen JH. Cremophor EL causes (pseudo-) non-linear pharmacokinetics of paclitaxel in patients. Br J Cancer. 1999;81:330–5.

33. Gelderblom H, Verweij J, van Zomeren DM, Buijs D, Ouwens L, Nooter K, *et al.* Influence of Cremophor El on the bioavailability of intraperitoneal paclitaxel. Clin Cancer Res. 2002;8:1237–41.
34. Kearns CM, Gianni L, Egorin MJ. Paclitaxel pharmacokinetics and pharmacodynamics. Semin Oncol. 1995;22:16–23.
35. van den Bongard HJ, Mathot RA, van Tellingen O, Schellens JH, Beijnen JH. A population analysis of the pharmacokinetics of Cremophor EL using nonlinear mixed-effect modelling. Cancer Chemother Pharmacol. 2002;50:16–24.
36. van Zuylen L, Gianni L, Verweij J, Mross K, Brouwer E, Loos WJ, *et al.* Inter-relationships of paclitaxel disposition, infusion duration and cremophor EL kinetics in cancer patients. Anticancer Drugs. 2000;11:331–7.
37. Lopez-Berestein G, Kasi L, Rosenblum MG, Haynie T, Jahns M, Glenn H, *et al.* Clinical pharmacology of 99mTc-labeled liposomes in patients with cancer. Cancer Res. 1984;44:375–8.
38. Sparreboom A, van Tellingen O, Huizing MT, Nooijen WJ, Beijnen JH. Determination of polyoxyethyleneglycerol triricinoleate 35 (Cremophor EL) in plasma by pre-column derivatization and reversed-phase high-performance liquid chromatography. J Chromatogr B Biomed Appl. 1996;681:355–62.
39. Mager DE, Jusko WJ. General pharmacokinetic model for drugs exhibiting target-mediated drug disposition. J Pharmacokinet Pharmacodyn. 2001;28:507–32.
40. Oeltmannand T, Frankel A. Advances in immunotoxins. FASEB J. 1991;5:2334–7.
41. Abraxis Bioscience. Nanoparticle albumin bound (nab) technology: A nanotechnology platform for biologically interactive drug delivery and targeting. FDA Briefing Document 06n0107/06n-0107-ts00015-Desai.ppt, FDA Oncologic Drugs Advisory Committee Meeting September 7, 2006. Available from: www.fda.gov/ohrms/dockets/dockets/06n0107/06n-0107-ts00015-Desai.ppt.
42. Henningsson A, Karlsson MO, Vigano L, Gianni L, Verweij J, Sparreboom A. Mechanism-based pharmacokinetic model for paclitaxel. J Clin Oncol. 2001;19:4065–73.
43. Henningsson A, Sparreboom A, Sandstrom M, Freijs A, Larsson R, Bergh J, *et al.* Population pharmacokinetic modelling of unbound and total plasma concentrations of paclitaxel in cancer patients. Eur J Cancer. 2003;39:1105–14.
44. Huizing MT, Keung AC, Rosing H, van der Kuij V, ten Bokkel Huinink WW, Mandjes IM, *et al.* Pharmacokinetics of paclitaxel and metabolites in a randomized comparative study in platinum-pretreated ovarian cancer patients. J Clin Oncol. 1993;11:2127–35.
45. Food and Drug Administration. Introduction or Stagnation: Challenge and Opportunity on the Critical Path to New Medical Products. Available from: http://www.fda.gov/ScienceResearch/SpecialTopics/CriticalPathInitiative/CriticalPathOpportunitiesReports/ucm077262.htm.
46. Paal K, Muller J, Hegedus L. High affinity binding of paclitaxel to human serum albumin. Eur J Biochem. 2001;268:2187–91.
47. US Food and Drug Administration - Center for Drug Evaluation and Research. FDA Briefing Document 2006-4235S2-02-01-FDAAbraxane.ppt. FDA Oncologic Drugs Advisory Committee Meeting September 7, 2006. Available from: http://www.fda.gov/ohrms/dockets/ac/06/slides/2006-4235S2-02-01-FDAAbraxane.ppt.
48. Nabholtz JM, Gelmon K, Bontenbal M, Spielmann M, Catimel G, Conte P, *et al.* Multicenter, randomized comparative study of two doses of paclitaxel in patients with metastatic breast cancer. J Clin Oncol. 1996;14:1858–67.
49. Friberg LE, Henningsson A, Maas H, Nguyen L, Karlsson MO. Model of chemotherapy-induced myelosuppression with parameter consistency across drugs. J Clin Oncol. 2002;20:4713–21.